



# EXPERIMENTAL INVESTIGATION ON INTEGRATED WICKLESS HEAT PIPE FOR SOLAR WATER HEATING

Ahmed Jabbar Hasan and Mohammed Hasan Abood  
Department of Mechanical Engineering, Karbala University, Karbala, Iraq  
E-Mail: [almussawie@yahoo.com](mailto:almussawie@yahoo.com)

## ABSTRACT

An integrated shape wickless heat pipe (WHP) inserted in flat plate solar collector (FPSC) is built and tested experimentally by a solar simulation using halogen projectors. The WHP made of copper with multi evaporator tubs and single horizontal condenser tube. It was tested for various evaporator diameter with distilled water as working fluid of fill ratios (40, 60, and 80) % and (450, 650, and 850) W/m<sup>2</sup> input heat flux to the solar collector at (30, 50, 70, and 90)<sup>0</sup> inclined angles. Results show that evaporator temperature and heat transfer coefficients are increase with input heat flux while thermal resistance decreases. Fill ratio have the direct effect on WHP performance and collector efficiency.

**Keywords:** wickless heat pipe, thermosyphon, solar simulation, flat plate collector.

## List of symbol

A: Surface area [m<sup>2</sup>]  
cp: Specific heat at constant pressure[J/kg.K]  
d: Diameter[m]  
FPSC: Flat Plate Solar Collector  
FR: Working fluid fill charge ratio (of evaporator volume)[%]  
h: Heat transfer coefficient [W/m<sup>2</sup>.K]  
I: Solar Insolation (radiation intensity)[W/m<sup>2</sup>]  
K: Thermal conductivity[W/m.K]  
L: Length[m]  
m<sup>0</sup>: Mass flow rate[kg/s]  
Q: Heat rate[W]  
Qu: Overall useful heat energy gain[W]  
q: Heat flux = Q/ A [W/m<sup>2</sup>]  
T: Temperature[<sup>0</sup>C]  
WHP: Wickless heat pipe

ev: Evaporator  
i: Internal  
l: Liquid  
o: Outer  
p: Plate  
s: Surface  
sat: Saturation  
t: Total, top

## Greek symbols

α: Absorptivity  
β: Inclination angle from the horizontal[Degree]  
Δ: Difference  
ε: Emissivity  
η: Efficiency  
τ: Transmissivity

## Subscripts

A: Ambient  
co: Condenser

## INTRODUCTION

The WHP is one of the most efficient devices in the process of heat transfer where it's a passive device that doesn't need outside power to run, and have a simply structure with high capability of temperature control as heat transfer in a high rate over small temperature deference between its two ends[1, 2]. There are many types and design of heat pipe but all depend on the principle of latent heat of vaporization as a heat transfer mode. Where the work principle of any heat pipe include existence of a working fluid inside a container divided into evaporator and condenser sections (with an adiabatic section almost).The liquid in the evaporator section get heat from outsource to vaporize and move toward the condenser section due to vapor pressure difference, then reject heat to a heat sink condensing vapor in to liquid phase then condensed liquid driven back by a gravity force to evaporator zone for WHPs where the condenser is always hold above the evaporator section. The principle work for integrated WHP shown in Figure-1.

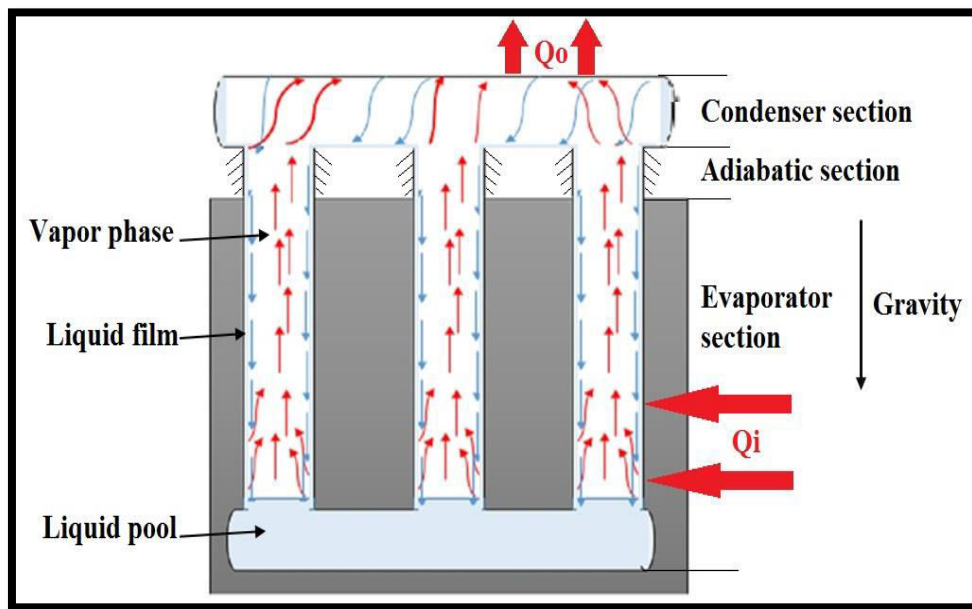


**Figure-1.**Wickless heat pipe work principle.

Many works study the effect of size, shape, working fluid, fill ratios, and inclined angles on the performance of WHPs.

Nioa, *et al.*[3,4] detected several parameters for WHP experimentally include fill ratio, input power, and aspect ratio using distilled water as working fluid. An isothermal evaporator temperature distribution was achieved from experiments. Later correlate empirical relation for boiling coefficient inside the WHP evaporator depending on the system pressure, heat flux, fill ratio, and aspect ratio. It give good agree with his experimental data and literature empirical relations.

While Jafari, *et al.*[5]studied the transient behavior of WHP by numerical simulation and experimental test, for purpose of maximum heat flux without dry out and geyser boiling phenomena. A WHP made of copper with internal diameter of 33mm and 500mm total length filled with water from 16 to 135% for heat input between the ranges of (30 to 700) W. They found that filling below 35% give better performance while the high fillings caused the geyser boiling.

Heat pipe working fluid studded by Ma, *et al.*[6]where they tested a WHP with eight refrigerant working fluids for renewable energy and find small differentiation between them.

Recently heat pipe heat exchanger is widely used in solar applications for its high thermal performance. And one of simplest and efficient application is the FPSC where the WHP role in the solar collector is to replace the riser tubes and transmit heat energy absorbed by the collector plate into the agent fluid in a storage tank or heat exchanger.

Khairnasov and Naumova [7]study the heat pipe application to a solar system and find there is many types of heat pipe can be used in solar application. Each one has advantages and disadvantages but all types add a new thermal resistance to the solar system, so that adding a

heat pipe should increases efficiency or give a simplicity in assembly or other benefits to compensate its additional thermal resistance. Also it found that Thermosyphon has less thermal resistance than other heat pipes.

A comparison was made by Ordaz-Flores *et al.*[8]between natural circulated Thermosyphon flat plate solar collector and two phase close Thermosyphon system with the same geometry and conditions but the close system reject heat by a coil condenser heat exchanger contained by storage tank. R134a and acetone were used as working fluids. The R134a close cycle Thermosyphon show better results in addition to some advantage like avoiding frizzling, corrosion, fouling, and scaling problems.

Azad[9] proposed a comparative method for testing flat plate solar collectors with different shape to absorb and extracted heat by installed them in parallel positions and integrated the heat pipes as a single heat pipe.

Some research for new shapes take only the general performance without study parameters change effect. Also outdoor testing doesn't give accurate comparison especially for solar application since it's effected by other environment parameters such as variation in solar radiation, wind speed, shade effect, and other non-controlled variables that may cause un right judgment on one of the studded parameters.

Some research for new shapes take only the general performance without study parameters change effect. Also outdoor testing doesn't give accurate comparison especially for solar application since it's effected by other environment parameters such as variation in solar radiation, wind speed, shade effect, and other non-controlled variables that may cause un right judgment on one of the studded parameters.

In the present work testing integrated WHP for FPSC by solar simulation and study the effect of fill ratio,



diameter of evaporator tubes, input heat flux in solar range, and system inclined angle on the performance of WHP in laboratory under steady conditions.

### Experimental apparatus and test procedure

Figure-2 represent experimental setup of WHP solar system. Where an integrated multi - branch evaporator consist of (12) cylindrical copper tubes connected together from the bottom by (elbow and T section joints) to form the evaporator structure. In this method the liquid is distributed evenly into each tube. that leads to made the WHP evaporator operate as a single system with regular distribution of heat transfer process and reduce the problems caused by dry out limitation as there is always liquid in the bottom to compensate if any tube test drying. The system, which contains an adiabatic section, is connected from the top by a horizontal tube as a condenser, with a diameter larger than the evaporator tubes to increase the surface area of the condenser. The horizontal shape enables to around it by other tube to concentrate a double pipe heat exchanger.

Two of WHPs was belted with outer evaporator tubes diameters of (19mm WHP1, and 16mm WHP2) with 1mm thickness for both WHPs evaporator tubes. Hence the bottom joints take the same diameter for each WHP with 40mm distance between tubes. The evaporator length was 900mm separate by 85mm adiabatic section from condenser tube of (720, 25.4, and 28) mm length, inner

and outer diameter respectively for both WHPs. The condenser is surrounded by a 60 mm diameter pipe for coolant fluid flow and covered as well as adiabatic section by 50mm thickness glass wool insulation to prevent heat losses to ambient.

The WHPs inserted to a FPSC of aluminum absorber plate of dimensions (920,740, and 1) mm length, width, and thickness respectively and covered by 4 mm thick glass window contained in wood casing box insulated from bottom and edges by 50mm thickness glass wool. A solar simulation was applied using halogen projectors to generate radiation energy. It can be easily move to give the required amount of radiation fall on the collector cover in regular manner.

When instilling a WHP to the FPSC it charged with distilled water at (40, 60, and 80) % of the evaporator internal volume, before charging it was vacuumed under heating using vacuum pump to remove the undesirable non- condensable gases that may exist in two forms either be a free gas or as molecules adsorbed on the metal surface. And after charging it also vacuumed and for equal time periods to arrive the saturation temperature required. Heat applied from (450 to 850)  $\text{W/m}^2$  at deferent inclined angles namely (30, 50, 70, and 90) $^\circ$  while water at 12  $^\circ\text{C}$  fixed inlet temperature with 0.65 L/min flow rate used as coolant fluid in the condenser section driven by emergent pump in 1000 L tank in open cycle

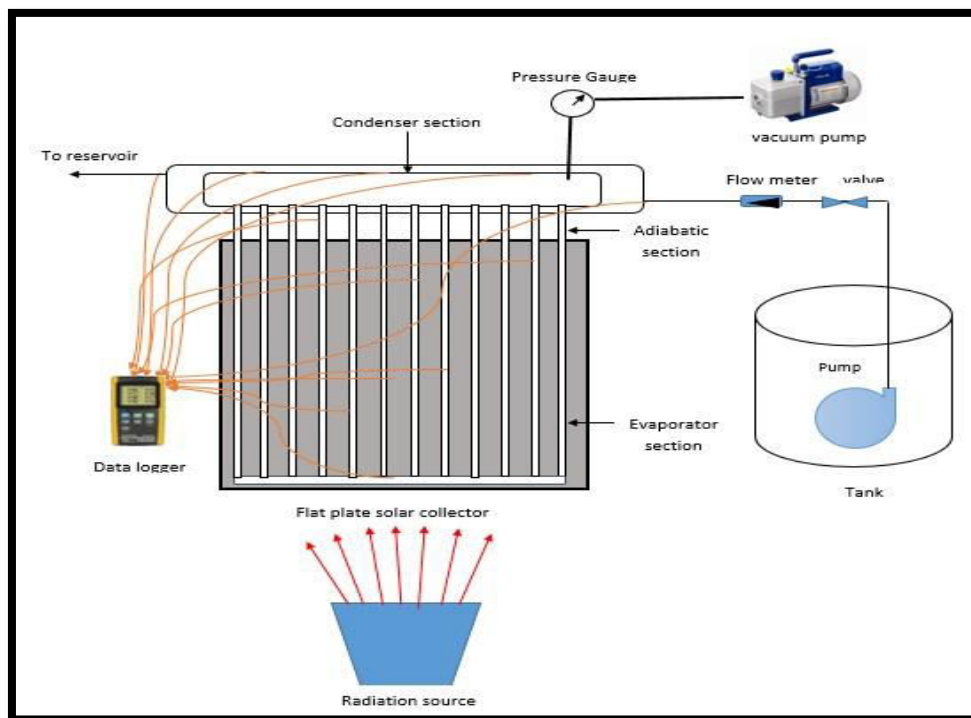


Figure-2.Experimental rig setup.

Firstly both WHPs tested at 90 $^\circ$  angle for all fill ratios and input powers. Then WHP1 tested at different inclined angles. The period of each experiment was about 2 hours, while the steady state was gated after about 25-30

minutes. All experiments repeated many times to ensure the results.



### Experimental measurements and calculations

The temperature distribution on different locations of WHP solar system measured by thermocouples wire type K with semi spherical head. It was used to contact with grooves made on the WHPs surface and at plate, inlet, and outlet of coolant to measuring the required temperatures. The thermocouples locations shown in Figure-3. They connected from the other side to a 12 channels temperature recorder (BTM-4208SD) with accuracy =  $\pm 0.4\%$ , Resolution =  $0.1^\circ$ , Reading temperature range of  $-100^\circ\text{C}$  to max. Temperature of  $1300^\circ\text{C}$ .

The incident power radiation on the collector is measured by a solar power meter type (TES 1333R) with a range changed from (0 to  $2000\text{ W/m}^2$ ), with resolution of  $0.1\text{ W/m}^2$ , accuracy  $\pm 10\text{ W/m}^2$ , and medium temperature range from (0 to  $50^\circ\text{C}$ ). The constant flow rate of coolant measured by a flow meter Sp.Gr.1.0.

Assumptions considered in the calculations of WHP on the FPSC system:

- Steady state heat transfer process in axial and radial directions.
- The radiation intensity applied on the collector cover is constant and uniformly distributed between the evaporator tubes.
- Neglecting bottom and edge losses and the contact resistance between plate and evaporator surface.
- The WHP is working at saturation temperature which determine the properties of the working fluid.
- The liquid vapor interface thermal resistance is neglected for both evaporator and condenser.
- The conduction in axial direction have slight effect on heat transfer so can be neglected.
- Neglect any loss in adiabatic and condenser section (assume perfect insulation).

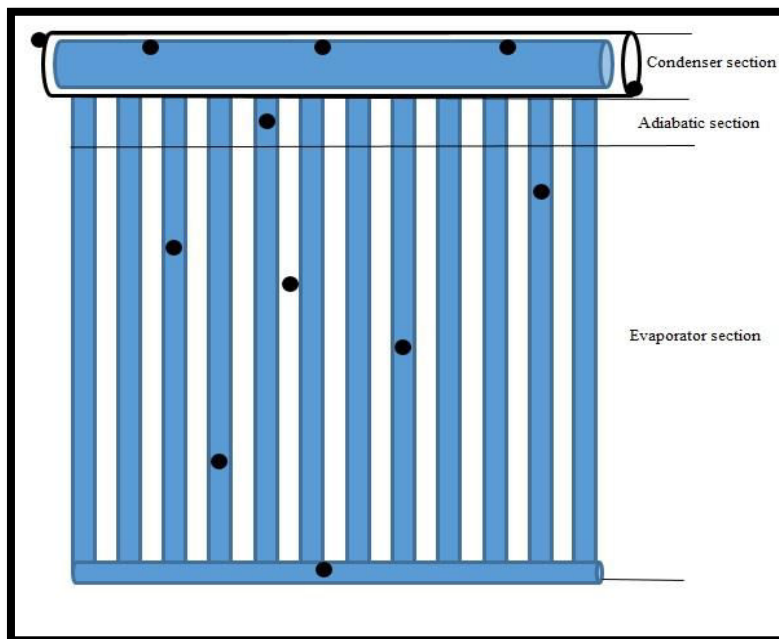


Figure-3. Thermocouple locations.

The heat input to the collector was calculating using the relation [10]

$$Q = IA_c(\tau\alpha)(1)$$

And collector losses is equal to [10]:

$$Q_L = U_t A_c (T_p - T_a)(2)$$

Where  $U_t$  from [11]

$$U_t = \left[ \frac{N_g}{\frac{C}{T_p} \left[ \frac{T_p - T_a}{N_g + f} \right]^{0.33} + \frac{1}{h_w}} \right]^{-1} + \frac{\sigma(T_p + T_a)(T_p^2 + T_a^2)}{\frac{1}{\varepsilon_p + 0.05N_g(1 - \varepsilon_p)} + \frac{2N_g + f - 1}{\varepsilon_g} - N_g} \quad (3)$$

$$f = (1 - 0.04h_w + 0.0005h_w^2)(1 + 0.091N_g)$$

$$C = 365.9(1 - 0.00883\beta + 0.0001298\beta^2)$$

$$h_w = \max \left[ 5, \frac{8.6V^{0.6}}{L^{0.4}} \right]$$

The wind heat transfer coefficient is taken 5 ( $\text{W/m}^2 \cdot ^\circ\text{C}$ ) for still air condition as in laboratory test.

The heat input to the evaporator section is:

$$Q_i = Q - Q_L \quad (4)$$

And in thermal resistance it equal to:

$$Q_i = \frac{T_{ev} - T_{co}}{R_t} \quad (5)$$



Where the total resistance of the WHP is:

$$R_t = R_{evw} + R_{evi} + R_{coi} + R_{cow} \quad (6)$$

Where

The evaporator and condenser wall resistance are:

$$R_{evw} = \frac{\ln(d_o/d_i)_{ev}}{2\pi L_{ev} K_w} \quad (7)$$

$$R_{cow} = \frac{\ln(d_o/d_i)_{co}}{2\pi L_{co} K_w} \quad (8)$$

The evaporator internal resistance

$$R_{evi} = \frac{1}{A_{ev} h_{ev}} \quad (9)$$

And condenser internal resistance

$$R_{coi} = \frac{1}{A_{co} h_{co}} \quad (10)$$

Evaporator, Condenser heat transfer coefficients are:[3, 12]

$$h_{ev} = \frac{Q_{ev}}{A_{ev} * (T_{ev} - T_v)} \quad (11)$$

$$h_{co} = \frac{Q_{co}}{A_{co} * (T_v - T_{co})} \quad (12)$$

Hence the evaporator and condenser temperatures taken as the average surface temperature for each one and vapor temperature is taken as the adiabatic surface temperature.

The useful heat gain is calculated from

$$Q_u = m c_p \Delta T \quad (13)$$

Where  $\Delta T$  is the temperature difference between the outlet and inlet of the coolant water.

Finally the collector efficiency is:[10]

$$\eta = \frac{Q_u}{I A_c} \quad (14)$$

## RESULTS AND DISCUSSIONS

### A. Temperature distribution along WHP and collector plate temperature

Figure-4 shows the temperature distribution of the WHP1 along the axial distance for different fill ratios and input heat flux to the collector. At the evaporator section (from 2 to 90 cm axial distance) liquid pool zone and vapor-liquid film zone appears. The liquid pool zone is higher temperature than the isothermal region of vapor-

liquid film. The initial value of liquid pool zone height also differs from its initial value according to its initial filling and heat flux.

A small difference in temperatures between the evaporator ends and adiabatic section while a temperature gradient become so clear between adiabatic and condenser section. This gradient is due to the internal thermal resistance of the WHP and its represent the driving force between condenser and evaporator.

The overall operating temperature increases with increasing the fill ratio, but the increase in evaporator temperature is larger than the increase in condenser temperature, since the condenser section effected directly by the coolant which has constant inlet temperature rather than heat input to evaporator or working fluid amount. The fill ratio of 40% shows the lower evaporator temperatures; also the isothermal performance is clearer in this fill ratio that because of continues vapor-liquid flow. The other small evaporator diameter WHP2 shows the same behavior but its run at temperature higher than WHP1 as clarified in Figure-5 for the 40% fill ratio and deferent input heat flux.

Figure-6 clarified the temperature distribution for WHP1 at different inclined angles at 650W/m<sup>2</sup> heat flux and 40% fill ratio. Notes that the inclined angle has slight effect on temperature distribution, however the angle of 30° has the lower temperature distribution but it's less than 2°C deference from other angles (50, 70)°. Also note that the liquid pool for inclined WHP is higher than that of vertical position for the method of distribution and also it relate to the performance of the WHP since the larger vapor generated have the maximum deference in height from the initial liquid pool height.

Another comparison can be made for the collector plate temperature as shown in Figure-7. The plate temperature have examine large variation in values when the working fluid filling and evaporator diameter has changed for the same input power condition hence the 40% FR of WHP1 shows the lower plate temperatures at all input powers due its low evaporator thermal resistance. Generally plate temperature increases with the increasing of input heat flux and fill ratio, and decreases when evaporator tube diameter increases. In other hand for WHP1 at 40% FR and 650 W/m<sup>2</sup> Figure-8 clarified that inclined angle have less effect on plate temperature.

### B. Heat transfer coefficient and thermal resistance

Figure-9 represent experimental evaporator heat transfer coefficient against heat flux for vertical position. The maximum value of (410 W/m<sup>2</sup>.°C) achieved at 40% fill ratio for WHP1 at 850 W/m<sup>2</sup> input heat flux, while minimum value is (55 W/m<sup>2</sup>.°C) at 80% fill ratio of the small diameter (WHP2) at 450 W/m<sup>2</sup> input heat flux.

As indicated in equation (11) the experimental evaporator heat transfer coefficient directly proportion with the input heat flux and have inversely proportion with  $\Delta T_e$ , but the increase in the heat flux is more than the increase in  $\Delta T_e$ .

As shown in Figure-9 fill ratio is more effect on the evaporator coefficient since (260 W/m<sup>2</sup>.°C) deference





in boiling coefficient between two deferent fill ratios namely (40, 80) % for a constant heat flux, coolant flow rate, inlet temperature, and evaporator surface area. It is thought that because of the high required amount of energy for relatively high fill ratios.

In the other hand the WHP1 has better boiling coefficient than WHP2 since it larger surface area so it has lower thermal resistance between plate and tube from side and tubes with the working fluid from the other side.

Figure-10 shows effect of inclined angle on the evaporator heat transfer coefficient. Its value is lower than the vertical position due to the liquid pool, liquid-film distribution inside the evaporator internal surface. However there is slight difference between other inclined angles (30, 50, 70)<sup>0</sup>.

The condenser heat transfer coefficient is presented in Figure-11 for both WHPs. Its value is higher than evaporator heat transfer coefficient since  $\Delta T$  between vapor and condenser surface temperature is lower than the difference in evaporator section. So that condenser section has lower thermal resistance although it has surface area less than evaporator by ten times. However the 40 % FR has highest values since there is continuous vapor and liquid-film flow.

The total thermal resistance indicated in Figure-12 for both WHPs. It observed that it's decreasing with increasing input heat flux and evaporator diameter and the opposite with the fill ratio. Hence total resistance affected directly by evaporator thermal resistance than others resistance. A close value of total thermal resistance

observed at different inclined angles with lower value at 30<sup>0</sup> as shown in Figure-13.

### C. Useful heat gain and overall collector efficiency

Figures 14 and 15 represent the heat gain by WHP1 for various fill ratios at 850 and 450 W/m<sup>2</sup> respectively. The 40% FR has more steady operation than other fillings; it's expected that because of continuous liquid film and liquid pool. The other fillings exam a fluctuation in heat transfer due to sudden vapor generated in evaporator caused noise and vibration in the WHP structure that called the geyser boiling phenomena. A same result of heat gain and collector efficiency behavior with lower values observed from WHP2.

Figure-16 indicates the useful heat gain at different inclined angles at 40% FR and 650 W/m<sup>2</sup> for WHP1. The vertical position show higher and more steady operation. However the 30<sup>0</sup> is found suitable since its closer to the vertical position.

Overall collector efficiency at deferent heat fluxes and fill ratios for both WHPs indicated in Figure-17. The 40% FR shows highest efficiency than other fillings and for both WHPs with steady value at deferent heat input while the 60, 80% FR show lower collector efficiency especially at low heat flux. The WHP1 is higher efficiency than WHP2 for the same fill ratio and heat flux. Figure-18 shows that the 30<sup>0</sup> inclined angle has the nearest efficiency to the vertical position.

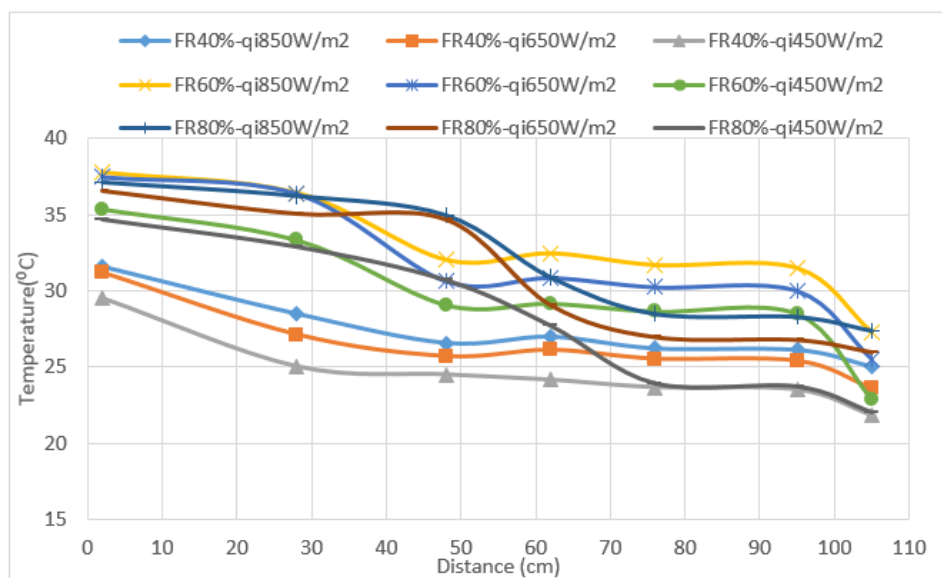
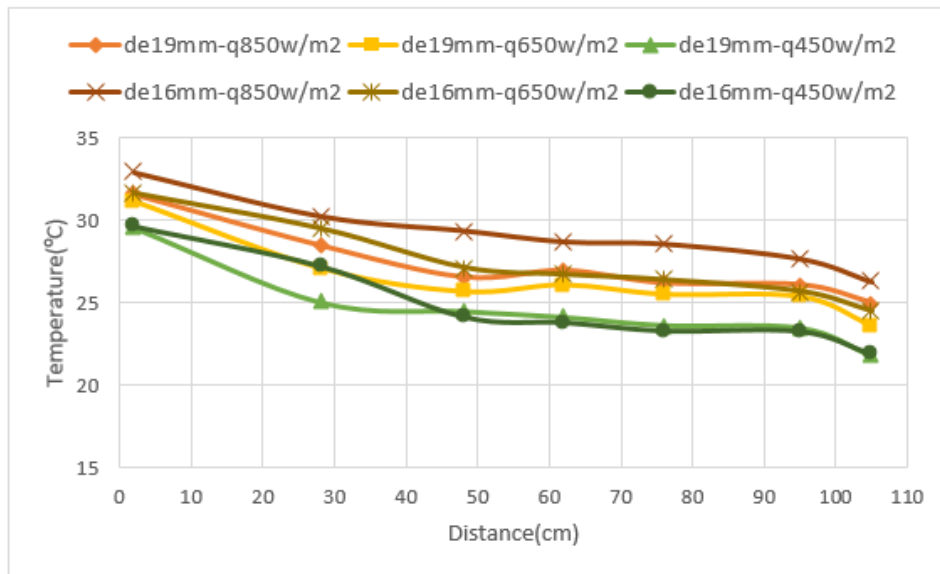
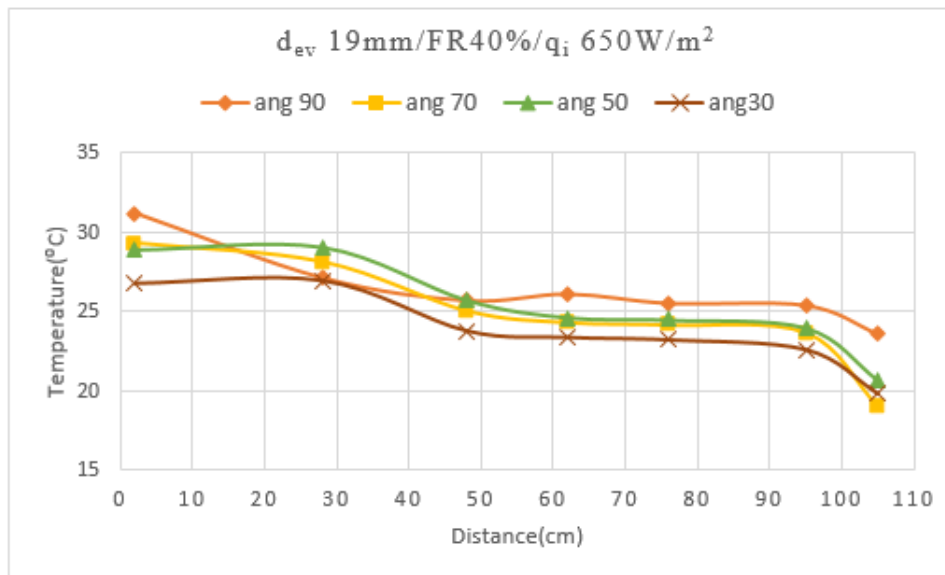


Figure-4. Temperature distribution along the axial distance of WHP1 at the vertical position.



**Figure-5.** Temperature distribution for both WHPs at the vertical position and 40% FR.



**Figure-6.** Temperature distribution of WHP1 at different inclined angles.

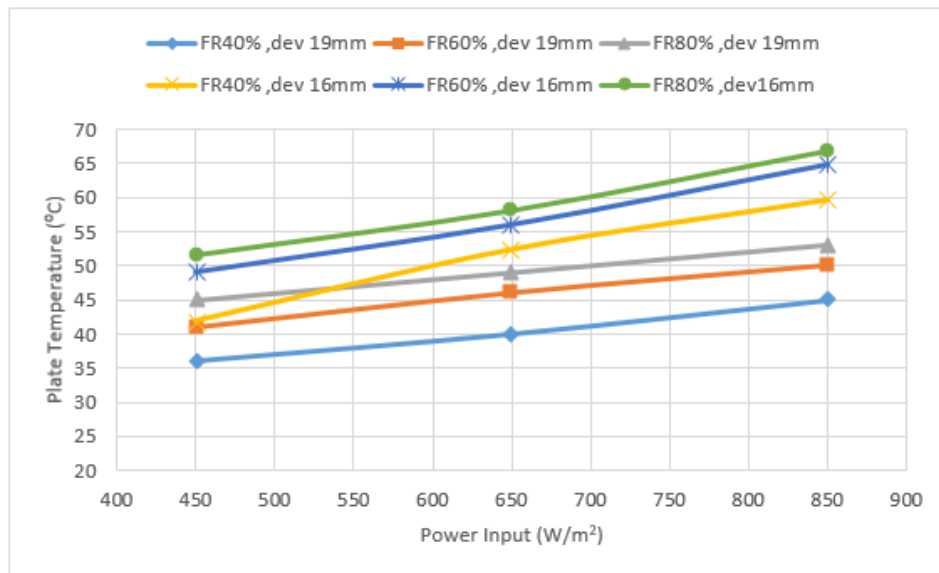


**Figure-7.** Absorbing plate temperatures at vertical position.

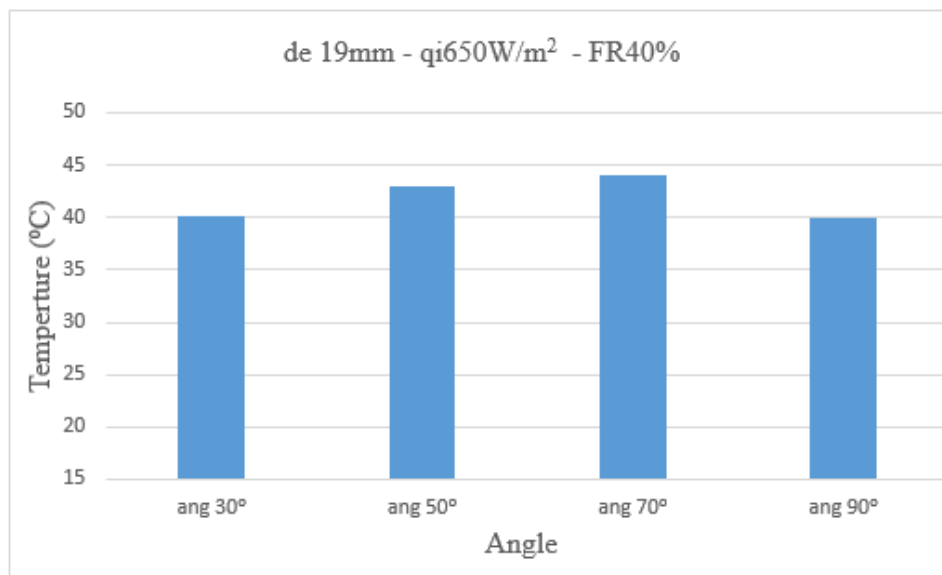


**Figure-8.** Plat temperature of WHP1 at different inclined angles.



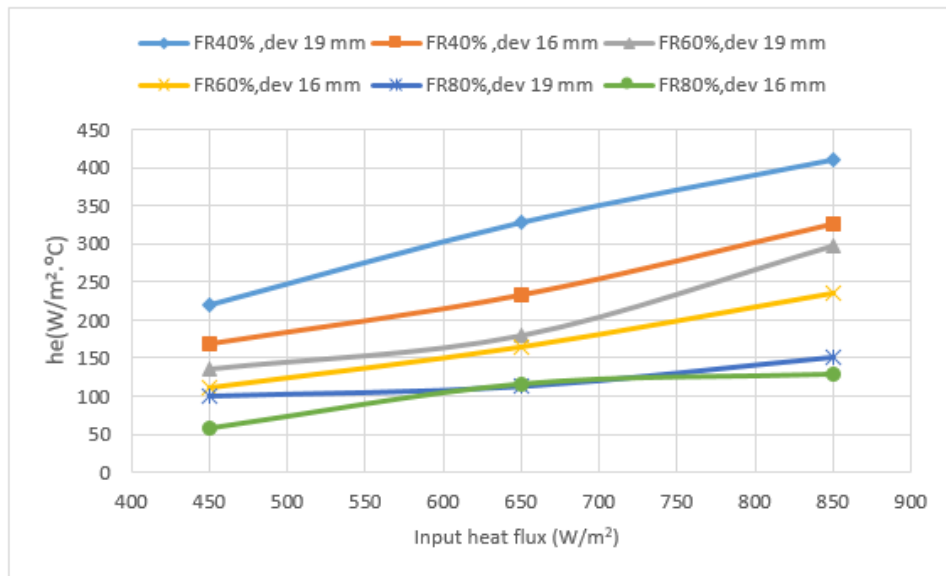


**Figure-9.**Evaporator heat transfer coefficient at different fills and input power at the vertical position.

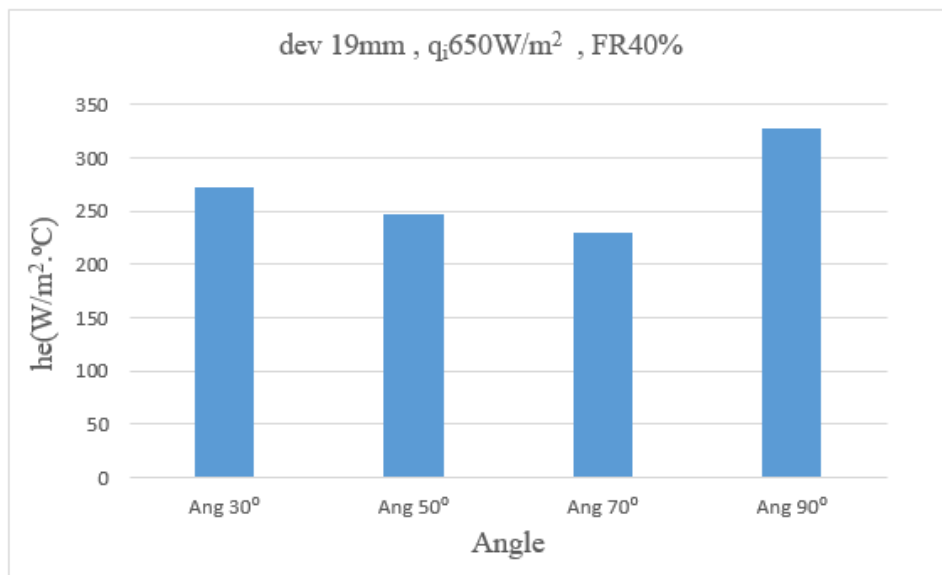


**Figure-10.**Evaporator heat transfer coefficient at different angles.

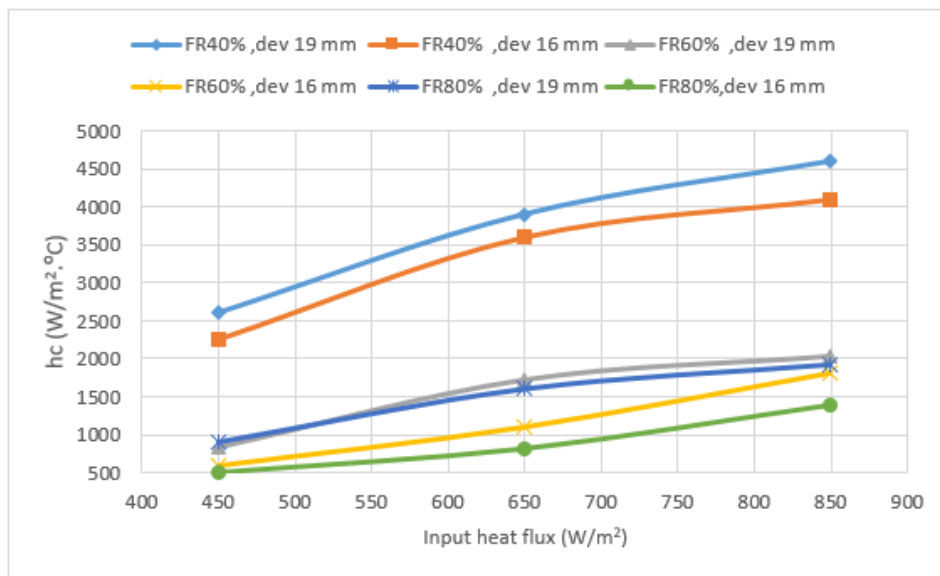


**Figure-11.**Condenser heat transfer coefficient for both WHPs at the vertical position.

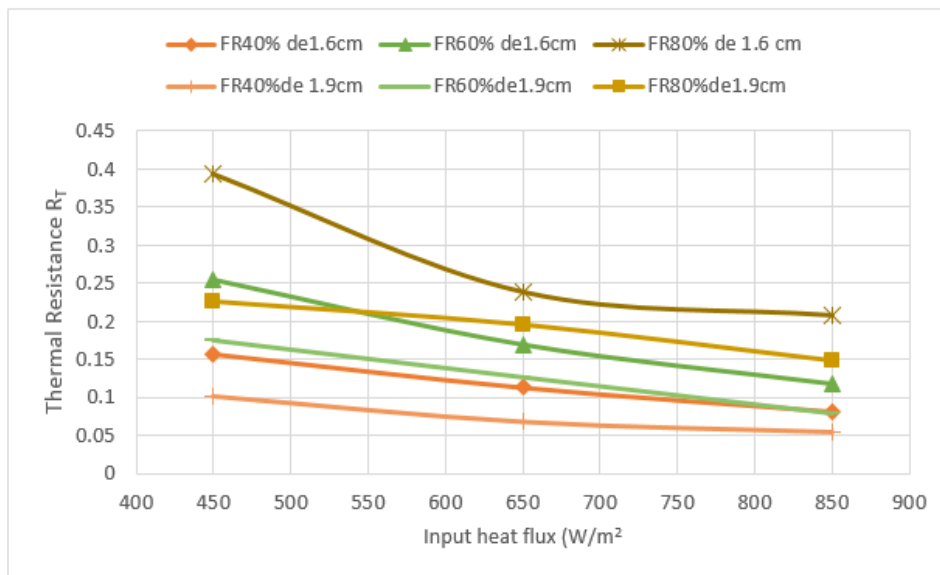


**Figure-12.**Total thermal resistance at the vertical position.

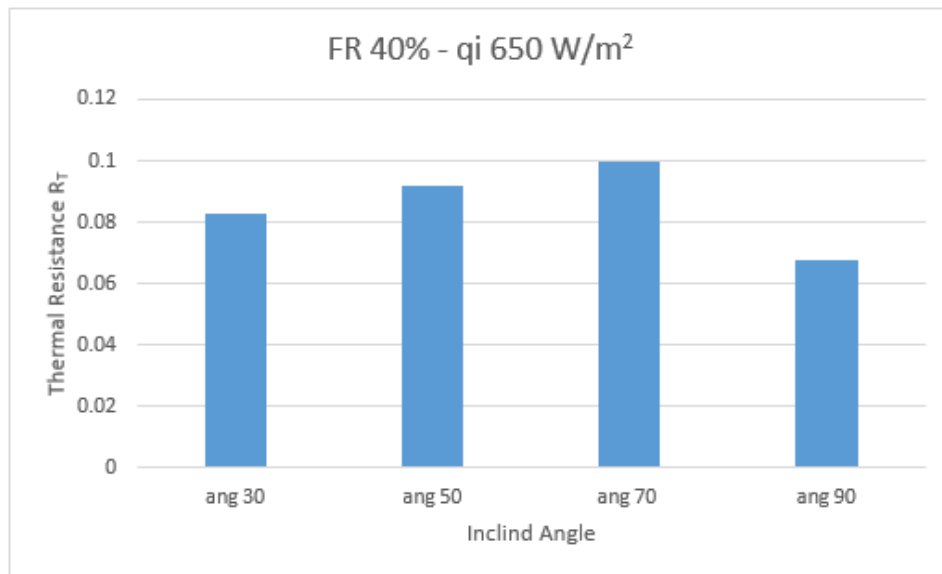


**Figure-13.**Total thermal resistance at different inclined angles for WHP1.

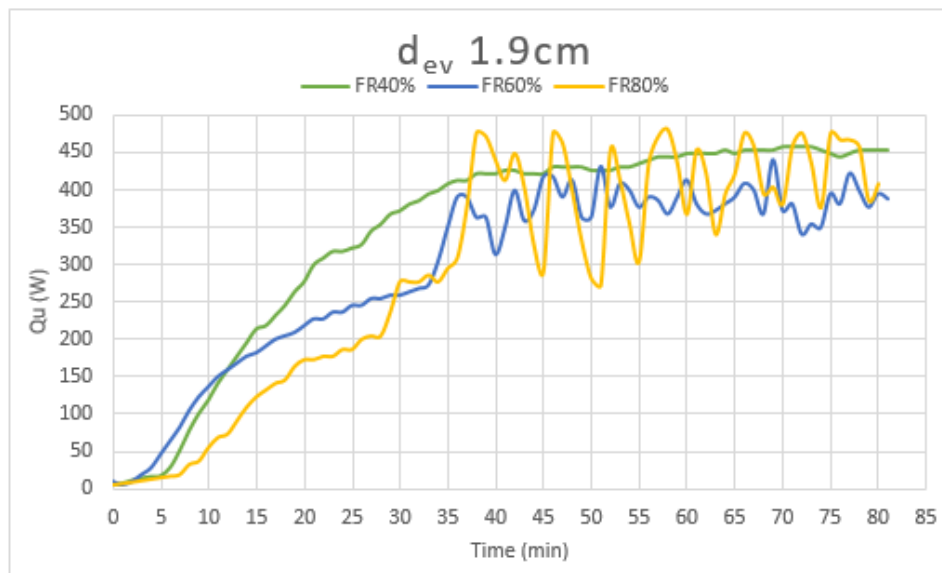


**Figure-14.**Useful heat gain for WHP1 at the vertical position and  $850\text{W/m}^2$  heat input.

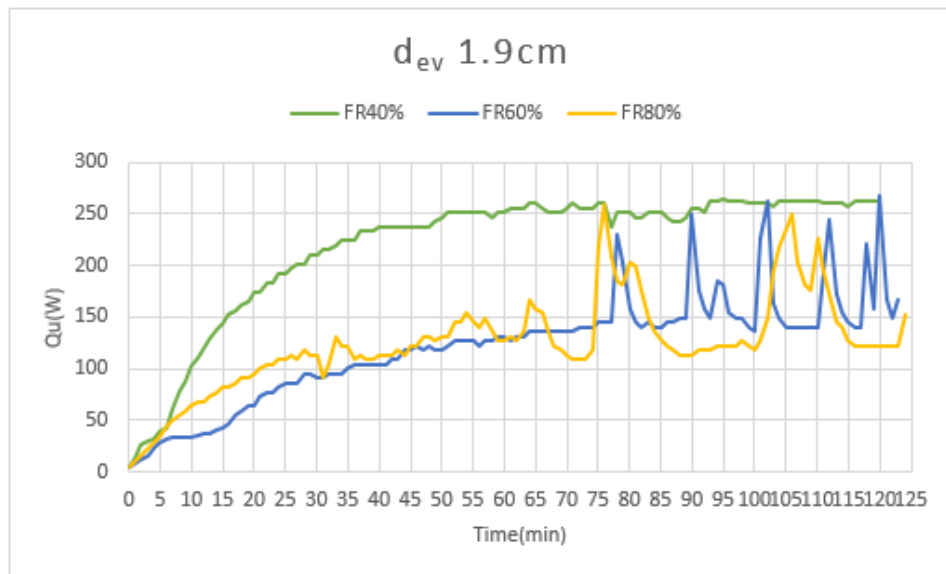


**Figure-15.** Useful heat gain for WHP1 at the vertical position and  $450\text{W/m}^2$  heat input.

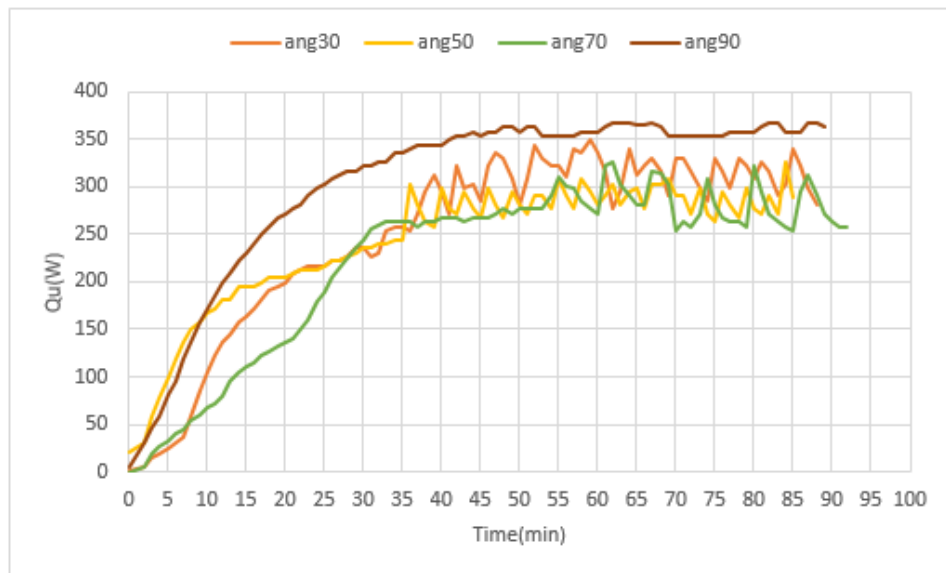


**Figure-16.** Useful heat gain for WHP1 at different inclined angles and  $650\text{W/m}^2$  heat input.

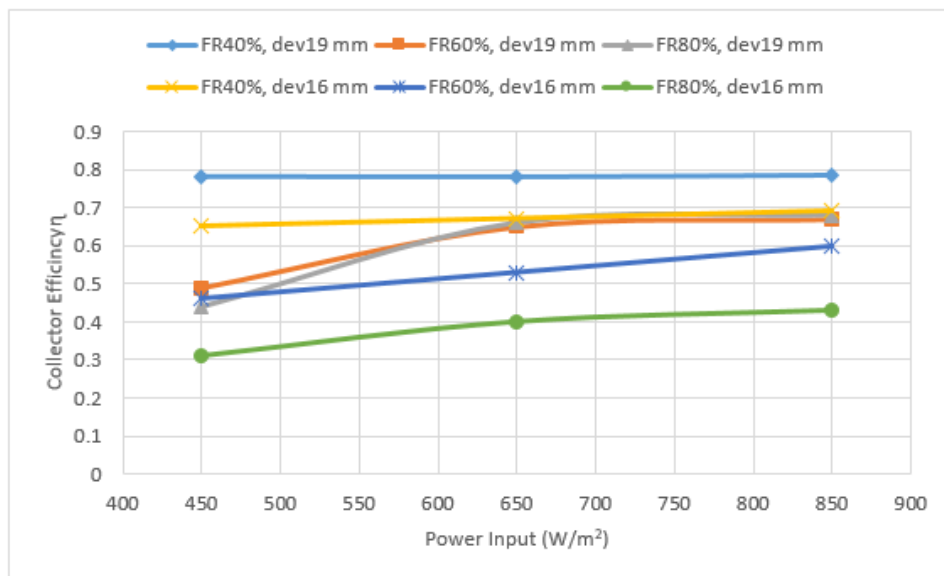


Figure-17. Overall collector efficiency for both WHPs at the vertical position.

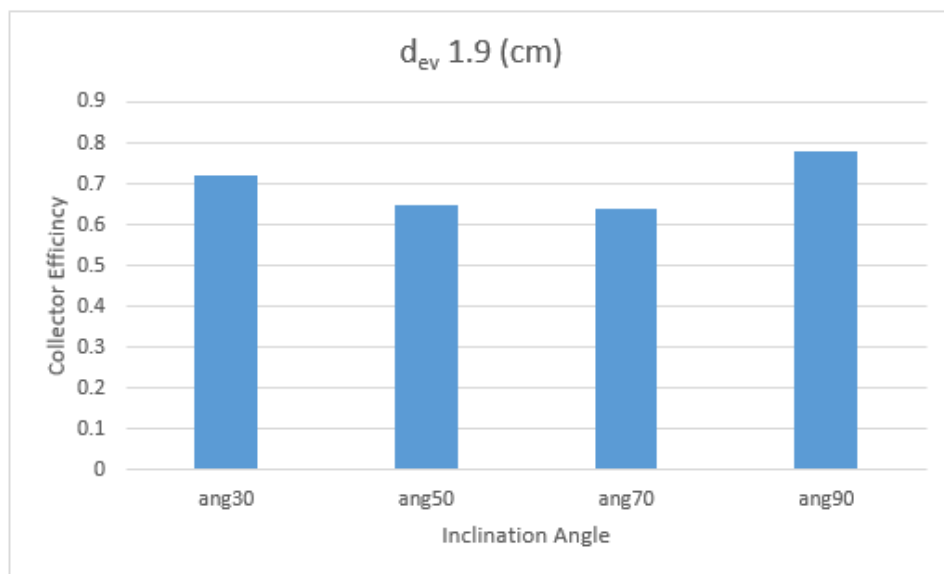


Figure-18. Overall collector efficiency for WHP1 at different inclined angles.

## CONCLUSIONS

From the laboratory results of testing two integrated WHPs for FPSC with different evaporator diameter and constant condenser diameter by a solar simulation using halogen projectors as radiation source and for constant inlet temperature and flow rate of coolant fluid at different fill ratios (40, 60, and 80) % and input heat flux (450, 650, and 850) W/m<sup>2</sup> at (30, 50, 70, and 90)<sup>0</sup> inclined angles the following conclusions can be driven:

- Testing a solar application by laboratory solar simulation give good vision of its performance especially at small differences
- The 40% fill ratio maintains the evaporator of the WHP and absorber plate at lower temperature, and closer to condenser temperature.

- Evaporator heat transfer coefficient increases with input heat flux and evaporator diameter. And depend mainly on initial fill charge ratio of working fluid.
- Increasing input heat flux and evaporator diameter lowered the total thermal resistance.
- The 30<sup>0</sup> inclined angles show the nearest performance of WHP to the vertical position.
- The 40% fill ratio give steady performance for maximum heat transfer without dry out or geyser boiling phenomena which observed at high fill ratios
- The integrated WHP give relatively high efficiency for the FPSC.

## REFERENCES

- Faghri A. 2014. Heat pipes: review, opportunities and challenges. *Frontiers in Heat Pipes (FHP)*. 5(1).



- [2] Reay D., R. McGlen and P. Kew. 2013. Heat pipes: theory, design and applications, ed. s. edition. Butterworth-Heinemann.
- [3] Noie S. 2005. Heat transfer characteristics of a two-phase closed thermosyphon. *Applied Thermal Engineering*. 25(4): 495-506.
- [4] Noie S., M. Kalaei and M. Khoshnoodi. 2005. Experimental investigation of boiling and condensation heat transfer of a two phase closed thermosyphon. *International Journal of Engineering*. 18(1): 37-43.
- [5] Jafari Davoud., Filippeschi Sauro., Franco Alessandro and Di Marco Paolo. 2017. Unsteady experimental and numerical analysis of a two-phase closed thermosyphon at different filling ratios. *Experimental Thermal and Fluid Science*. 81: 164-174.
- [6] Ma Limin., Shang Linlin., Zhong Dan. and Ji Zhongli. 2017. Experimental Performance of a Two-phase Closed Thermosyphon Charged with Hydrocarbons and Freon Refrigerants for Renewable Energy Applications. *Energy Procedia*. 105: 5147-5152.
- [7] Khairnasov S. and A. Naumova. 2016. Heat pipes application to solar energy systems. *Applied Solar Energy*. 52(1):47.
- [8] Ordaz-Flores A., O. García-Valladares and V. Gómez. 2009. Evaluation of the Thermal Performance of a Solar Water Heating Thermosyphon versus a Two-Phase Closed Thermosyphon Using Different Working Fluids. in *Proceedings of ISES World Congress 2007 (Vol. I-Vol. V)*. Springer.
- [9] Azad E. 2012. Assessment of three types of heat pipe solar collectors. *Renewable and Sustainable Energy Reviews*. 16(5): 2833-2838.
- [10] Duffie J.A. and W.A. Beckman. 2013. *Solar engineering of thermal processes*. John Wiley & Sons.
- [11] Kalogirou S.A. 2013. *Solar energy engineering: processes and systems*. Academic Press.
- [12] Eidan A.A., S.E. Najim and J.M. Jalil. 2016. Experimental and numerical investigation of thermosyphone performance in HVAC system applications. *Heat and Mass Transfer*. 12(52): 2879-2893.
- [13] Jiao B., Qiu LM. Zhang XB and Zhang Y. 2008. Investigation on the effect of filling ratio on the steady-state heat transfer performance of a vertical two-phase closed thermosyphon. *Applied Thermal Engineering*. 28(11): 1417-1426.
- [14] Khazaei I., R. Hosseini and S. Noie. 2010. Experimental investigation of effective parameters and correlation of geyser boiling in a two-phase closed thermosyphon. *Applied Thermal Engineering*. 30(5): 406-412.
- [15] LinTF, Lin WT., Tsay YL., Wu JC. and Shyu RJ. 1995. Experimental investigation of geyser boiling in an annular two-phase closed thermosyphon. *International journal of heat and mass transfer*. 38(2): 295-307.